

The hydrolysis reaction of some cubic and tetragonal lanthanide dicarbide solid solutions

I. J. McColm

Department of Industrial Technology, University of Bradford, Bradford BD7 1DP (UK)

(Received October 5, 1992)

Abstract

Two series of solid solution dicarbides made from a light and a heavy dicarbide, $\text{Er}_{1-x}\text{Ce}_x\text{C}_2$ and $\text{Lu}_{1-x}\text{La}_x\text{C}_2$, have been made and the change in X-ray lattice parameters across the series of tetragonal and cubic phases determined. Deviations from Vegard's law behaviour are discussed. Both series have been hydrolysed in water vapour at $11.0 \times 10^2 \text{ Nm}^{-2}$ pressure and 14.5°C and the rate constants for the linear reaction determined. The reaction rates for the $\text{Lu}_{1-x}\text{La}_x\text{C}_2$ samples with water have been measured together with four cubic phases, $\text{Lu}_{0.5}\text{La}_{0.5}\text{C}_2$, $\text{Lu}_{0.5}\text{Ce}_{0.5}\text{C}_2$, $\text{Lu}_{0.5}\text{Pr}_{0.5}\text{C}_2$ and $\text{Lu}_{0.5}\text{Nd}_{0.5}\text{C}_2$. The changes in linear reaction rate constants for these samples, together with those of CeC_2 and LuC_2 , are discussed in terms of C–C bond lengths and f character of the metal band electrons which contribute to the M–C₂ covalent bond. The reactivity sequence $\text{CeC}_2 > \text{Ce}_{0.5}\text{Lu}_{0.5}\text{C}_2 \gg \text{LuC}_2$ is explained.

1. Introduction

Previous papers have described the work done to relate the hydrolysis reaction kinetics to hardness and structural parameters of tetragonal lanthanide dicarbides and some of their tetragonal solid solutions [1–4]. Some of the changes in reaction rates, in hardness, and their correlation with the f character of band electrons in the covalent part of the M–C₂ bond appeared to distinguish between the light lanthanides La–Nd and the heavy group Sm–Lu, with YC_2 having properties closer to GdC_2 than HoC_2 , to which it is closer in X-ray unit cell volume size [4]. In this paper some results are presented for two series of dicarbide solid solutions between members from these two groupings, $\text{Lu}_{1-x}\text{La}_x\text{C}_2$ and $\text{Er}_{1-x}\text{Ce}_x\text{C}_2$, together with some data for four $\text{Lu}_{0.5}\text{Ln}_{0.5}\text{C}_2$ cubic dicarbides, the aim being to probe further the factors that stabilize the cubic polymorph, which is normally the high temperature structure in dicarbide systems, down to room temperatures, and factors influencing the hydrolytic reactivity of both tetragonal and cubic phases.

The equations for the hydrolysis reactions and the definitions of mild conditions are set out in earlier papers of this series [1, 2].

2. Experimental details

All the preparative, characterization, and hydrolysis measurement techniques have been fully described be-

fore [1–5] and most of the solid solutions were prepared from the same stock dicarbide samples used in ref. 2.

3. Results

3.1. ErC_2 – CeC_2

For this system, as Fig. 1 shows, two tetragonal solid solution regions border a wide region where cubic solid solutions are stable to ambient temperatures. Figure 1 has been constructed by dividing the X-ray unit cell volume by the number of metal atoms in the unit cell. Considering the data in Fig. 1 in terms of the larger volume CeC_2 dissolving into ErC_2 , the solvent, they suggest that from ErC_2 to $\text{Er}_{0.8}\text{Ce}_{0.2}\text{C}_2$, linear Vegard behaviour occurs with ideal solid solution formation. However, up to the phase boundary, at $\text{Er}_{0.7}\text{Ce}_{0.3}\text{C}_2$, the solid solution behaviour is less than perfect as the metal atoms appear to account for more of the volume. This may indicate a sharper decline in the C–C distance of the $(\text{C}_2)^{2-}$ dipoles aligned along the [001] direction. This suggestion is supported by the way in which the c-axis length does not increase uniformly from $\text{Er}_{0.8}\text{Ce}_{0.2}\text{C}_2$ to $\text{Er}_{0.7}\text{Ce}_{0.3}\text{C}_2$ as the concentration of the larger cerium atom increases, as shown in Fig. 2, but rather a sharp increase in the a, b axes lengths is observed.

When a cubic sample of $\text{Er}_{0.7}\text{Ce}_{0.3}\text{C}_2$ composition was annealed in vacuum at 1150°C for 14 h, followed by slow furnace-cooling, it changed to the tetragonal

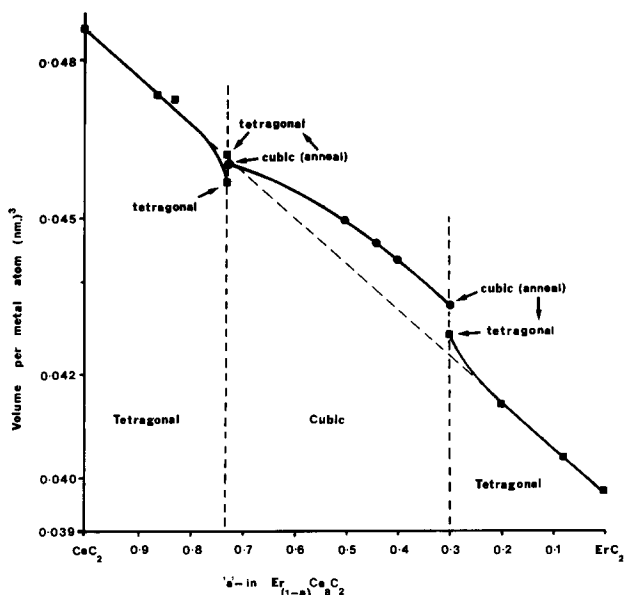


Fig. 1. The change in volume per metal atom in the X-ray unit cell for tetragonal and cubic solid solutions $\text{Er}_{1-x}\text{Ce}_x\text{C}_2$.

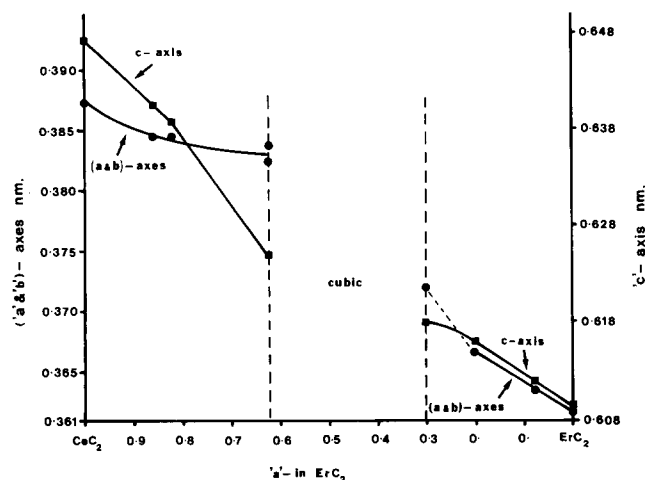


Fig. 2. X-ray unit cell a , b and c parameters for the tetragonal phases in the $\text{Er}_{1-x}\text{Ce}_x\text{C}_2$ system.

polymorph with an identical volume per metal atom as a tetragonal phase also identified at $\text{Er}_{0.7}\text{Ce}_{0.3}\text{C}_2$. No other cubic phases near to the $x=0.3$ boundary transformed on annealing.

Solid solutions across the cubic range do not exhibit a Vegard relationship but lie on a curve above the line connecting the solid solutions in the two tetragonal regions, as Fig. 1 indicates. Substitution of the erbium by cerium leads to larger X-ray unit cells than expected, which could be a result of increased C–C bond lengths. In Fig. 1 the drawing of the boundary at $\text{Er}_{0.265}\text{Ce}_{0.735}\text{C}_2$ is supported by the fact that an arc-cast sample of this composition produced a tetragonal phase below the Vegard line, which when annealed at 1100 °C for 14 h and then furnace cooled became two phase, one

cubic and one tetragonal, which had unit cells such that they gave volume per metal atom points close to the Vegard line shown in Fig. 1.

For the cerium-rich solid solutions, the change from tetragonal to cubic dicarbide appears, from Fig. 2, to be associated with a sharp decrease in the c axis parameter while the a , b axes are only slightly decreased.

Because varying percentages of Ce(IV) can be present in cerium-based dicarbides and this can affect the reaction rate data obtained from the evolved gas analysis method, the hydrolysis behaviour of the $\text{Er}_{1-x}\text{Ce}_x\text{C}_2$ phases was tested by the microbalance method at 14.5 °C and a water vapour pressure of $11 \times 10^2 \text{ Nm}^{-2}$. Data from these tests are shown in Table 1 but cannot be obviously interpreted, probably because of the overriding effect that the surface H_2O adsorption and coverage can have [1]. However, the sharply decreasing c axis parameter in the cerium-rich solutions, which indicates a shortening of the C–C bond length, and a resultant decrease in M–C₂ covalent bond strength give rise to a sharp increase in reactivity up to $6.7 \times 10^{-2} \text{ mg cm}^{-2} \text{ min}^{-1}$ for K_L , the linear reaction rate constant, for $\text{Er}_{0.38}\text{Ce}_{0.62}\text{C}_2$. The cubic phases are notable for the sharp drop in reaction rate constant values, and the second series of erbium-rich solid solutions again appear much more reactive.

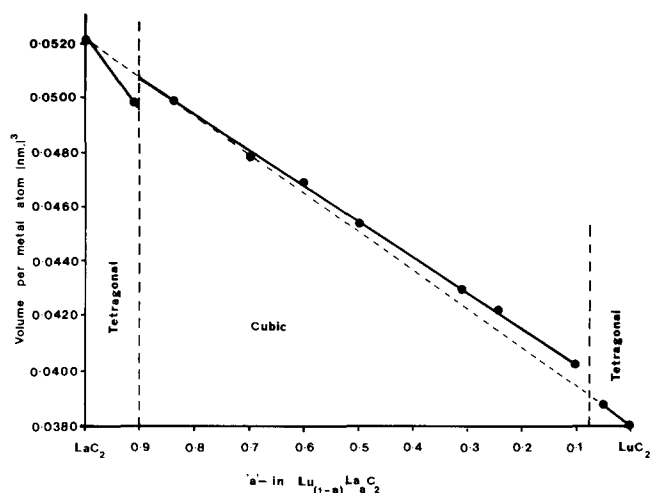
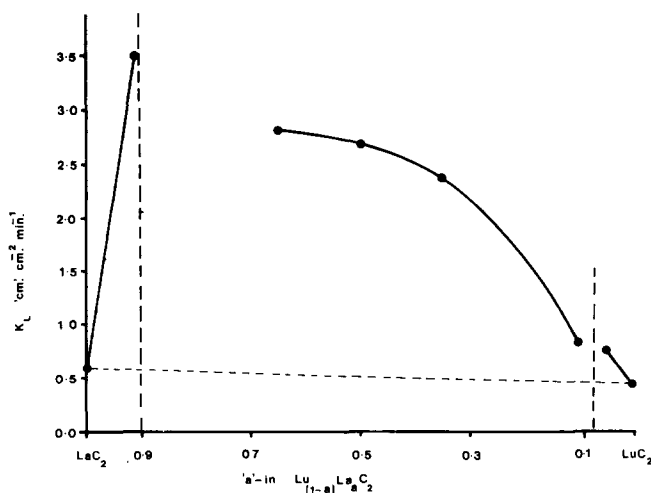
3.2. LuC_2 – LaC_2

The high temperature cubic polymorph is quickly stabilized to room temperature in this system, as Fig. 3 shows. The whole range from $\text{Lu}_{0.1}\text{La}_{0.9}\text{C}_2$ to $\text{Lu}_{0.925}\text{La}_{0.075}\text{C}_2$ is a cubic solid solution series. Again the transition from the tetragonal phases to the cubic phase is accompanied by an increase in volume per metal atom at the phase boundaries. Across the cubic phase range the solid solution behaviour appear to follow a perfect Vegard behaviour as far as the unit cell volume is concerned. When the reaction rate for the hydrolysis by water vapour is considered (Table 1), all the solid solutions exhibit enhanced reactivity compared with both LaC_2 and LuC_2 . The increased rate when 10% of lanthanum is substituted by lutetium is quite dramatic as was the case when a small erbium substitution was made in the $\text{Er}_{1-x}\text{Ce}_x\text{C}_2$ system. All cubic compositions in the $\text{Lu}_{1-x}\text{La}_x\text{C}_2$ series exhibit obvious increased reactivity compared with the tetragonal precursor dicarbides, which was in contrast to the results from the $\text{Er}_{1-x}\text{Ce}_x\text{C}_2$ series.

For the $\text{Lu}_{1-x}\text{La}_x\text{C}_2$ series of cubic solid solutions, because the uncertainty regarding the metal atom oxidation state, compared with those containing cerium, was removed, the samples were tested using liquid water as the reagent. This action removes the surface coverage with H_2O vapour stage as being rate determining and switches attention to the strength of the $\text{M}-(\text{C}_2)^n-$

TABLE 1. Variation in the linear reaction rate constant with composition for the reaction of water vapour at $11 \times 10^2 \text{ Nm}^{-2}$ pressure and 14.5°C for two series of dicarbide solid solutions

Composition	$K_L \times 10^2$ ($\text{mg cm}^{-2} \text{ min}^{-1}$)	Composition	$K_L \times 10^2$ ($\text{mg cm}^{-2} \text{ min}^{-1}$)
CeC_2	2.0	$\left\{ \begin{array}{l} \text{LaC}_2 \\ \text{La}_{0.9}\text{Lu}_{0.1}\text{C}_2 \end{array} \right.$	0.99
$\text{Ce}_{0.82}\text{Er}_{0.18}\text{C}_2$	5.2		7.70
$\text{Ce}_{0.62}\text{Er}_{0.38}\text{C}_2$	6.7	$\left\{ \begin{array}{l} \text{La}_{0.8}\text{Lu}_{0.2}\text{C}_2 \\ \text{La}_{0.5}\text{Lu}_{0.5}\text{C}_2 \\ \text{La}_{0.1}\text{Lu}_{0.9}\text{C}_2 \end{array} \right.$	11.70
$\text{Ce}_{0.50}\text{Er}_{0.50}\text{C}_2$	3.2		7.50
$\text{Ce}_{0.40}\text{Er}_{0.60}\text{C}_2$	2.7		5.4
$\text{Ce}_{0.30}\text{Er}_{0.70}\text{C}_2$	4.7	$\left\{ \begin{array}{l} \text{La}_{0.05}\text{Lu}_{0.95}\text{C}_2 \\ \text{LuC}_2 \end{array} \right.$	3.6
$\text{Ce}_{0.20}\text{Er}_{0.80}\text{C}_2$	4.6		2.9
$\text{Ce}_{0.10}\text{Er}_{0.90}\text{C}_2$	5.5		
ErC_2	6.0		

Fig. 3. Volume per metal atom in the unit cells of tetragonal and cubic dicarbides in the series $\text{Lu}_{1-x}\text{La}_x\text{C}_2$.Fig. 4. The linear reaction rate constant K_L for the reaction of $\text{Lu}_{1-x}\text{La}_x\text{C}_2$ dicarbides with water at 20°C .

bond [2]. Results are shown as Fig. 4, where the enhanced reactivity above the line joining the LaC_2 and LuC_2 reaction rates is obviously shown. All solid solutions tested, even the two tetragonal phases, exhibit increased reactivity and, as for the water vapour reaction, the most dramatic increase occurs in the sample with a small substitution of lanthanum by lutetium. Despite the evidence in Fig. 3 for a smooth volume change throughout the cubic range as substitution is made, the hydrolysis behaviour is clearly non-linear.

3.3. $\text{Lu}_{0.5}\text{Ln}_{0.5}\text{C}_2$ cubic phases

Each of the four light lanthanum, cerium, praseodymium and neodymium lanthanides produces sufficient lattice mismatch and resultant strain to prevent nucleation of the tetragonal phase when cooled from the melt and so it was possible to examine the effect of mismatch strain on the kinetics of the water hydrolysis reaction of a series of related cubic phases. The results are shown in Table 2 and as a plot of the square of the unit cell volume in Fig. 5. With the exception of the $\text{Lu}_{0.5}\text{Nd}_{0.5}\text{C}_2$ there is some correlation between the strain parameter and the observed hydrolysis reaction rate constant.

TABLE 2. Lattice parameters and hydrolysis reaction rate constant for some cubic solid solutions of LuC_2

Phase	Lattice parameter (nm)	K_L ($"\text{cm}^2 \text{ min}^{-1}$)	Volume per metal atom (nm^3)
$\text{Lu}_{0.5}\text{La}_{0.5}\text{C}_2$	0.5646	2.74	0.04499
$\text{Lu}_{0.5}\text{Ce}_{0.5}\text{C}_2$	0.5604	2.13	0.04400
$\text{Lu}_{0.5}\text{Pr}_{0.5}\text{C}_2$	0.5564	1.61	0.04306
$\text{Lu}_{0.5}\text{Nd}_{0.5}\text{C}_2$	0.5544	1.59	0.0426

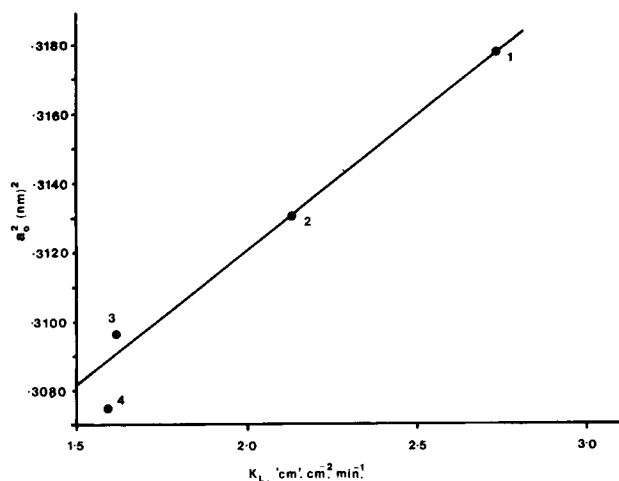


Fig. 5. A plot of the square of the cubic X-ray unit cell parameter against the observed linear rate constant at 20 °C for the reaction of $\text{Lu}_{0.5}\text{La}_{0.5}\text{C}_2$ (1), $\text{Lu}_{0.5}\text{Ce}_{0.5}\text{C}_2$ (2), $\text{Lu}_{0.5}\text{Pr}_{0.5}\text{C}_2$ (3) and $\text{Lu}_{0.5}\text{Nd}_{0.5}\text{C}_2$ (4) with water.

4. Discussion

The X-ray investigation of the two series of solid solutions both formed from a light lanthanide element and a heavy lanthanide show that transformation to the cubic phase is associated with a rapid decrease in the c -axis parameter accompanied by a more gradual increase, or even decrease, in the a , b axes, close to the phase boundaries. This effect is more easily reconciled with a $\langle 111 \rangle$ disorder model rather than a rotating $(\text{C}_2)^{n-}$ dipole model.

When the structural data are presented as a change in available volume per metal atom in the structure the way that the two tetragonal phases lie on a line connecting CeC_2 and ErC_2 , while the data points for the cubic phases lie above the line in Fig. 1 for example, seems significant. The samples very close to the phase boundaries do not lie on the connecting line and the non-linear plot through the cubic region suggests some disorder in these structures. The annealing behaviour of $\text{Er}_{1-x}\text{Ce}_x\text{C}_2$ samples at the tetragonal-cubic boundaries suggests that these boundaries have been exactly located in this system. This is not so true in the $\text{Lu}_{1-x}\text{La}_x\text{C}_2$ system where the very broad cubic phase range reveals a much less disordered situation in that linear behaviour is observed across the cubic region with many of the data points lying on or close to a Vegard relationship. A lack of f character in the band electrons in the La-Lu system, compared with the Ce-Er system, may be responsible for a difference. If that were the case then a much decreased reactivity might be expected in the $\text{Lu}_{1-x}\text{La}_x\text{C}_2$ solid solutions compared with the $\text{Er}_{1-x}\text{Ce}_x\text{C}_2$ series. The water vapour hydrolysis rate data in Table 2 do not support this hypothesis but of course the rate-determining step in such reactions

is probably more involved with surface coverage by H_2O vapour than with the $\text{M}-\text{C}_2$ bond strengths. Strain energy arising from atom size mismatch may also be important and would favour a greater reactivity for the La-Lu system where of course the strain from atom size mismatch is greater than in the Ce-Er system.

An attempt was made here to assess the strain effect by examining the water hydrolysis of $\text{Lu}_{0.5}\text{Ln}_{0.5}\text{C}_2$ cubic phases and as Fig. 5 indicates there may be a correlation between a volume function, the square of the mean volume of metal atoms per unit cell, and the observed linear reaction rate constant.

The C-C distances in the $(\text{C}_2)^{n-}$ dipoles of CeC_2 , $\text{Ce}_{0.5}\text{Lu}_{0.5}\text{C}_2$, and LuC_2 have recently been determined in a neutron study [6] and found to be 0.128 nm, 0.131 nm and 0.127₆ nm respectively. The longer the C-C bond then, the greater the $\text{M}-\text{C}_2$ covalent contribution to overall bonding as metal electrons occupy a band in which the C_2 π antibonding orbitals are part, and hence the order of reactivity in water might be expected to be $\text{CeC}_2 = \text{LuC}_2 > \text{Ce}_{0.5}\text{Lu}_{0.5}\text{C}_2$. The K_L values for these three carbides have been measured here as 6.9, 0.4, and 2.13 "cm" $\text{cm}^{-2} \text{min}^{-1}$, which has LuC_2 misplaced. However, when one recalls that the $\text{M}-\text{C}_2$ covalent bonding involves interaction between the C_2 $p\pi^*$ antibonding orbitals with a metal band of s , p , d and f character, then the relative contribution of the s , p , d and f states needs to be considered in the manner developed by Gschneidner [7]. Increased f character leads to weakening of the bond as shown by the melting points and hardness values of the light lanthanide compared with heavy members. Thus $\text{Ce}_{0.5}\text{Lu}_{0.5}\text{C}_2$ with the longest C-C bond has the most $p\pi^*$ -metal interaction, but since cerium is present there is an increased f character in the $\text{M}-\text{C}_2$ bond compared with LuC_2 and the solid solution is therefore approximately 5 times more reactive than LuC_2 . CeC_2 has a shorter C-C bond than the solid solution and more f band character and so the balance is to make it more reactive. The LuC_2 with no f electron character in the band is the most stable and the observed order of the reactivities is as expected.

References

- 1 I. J. McColm and T. A. Quigley, *J. Less-Common Met.*, 169 (1991) 347.
- 2 I. J. McColm, T. A. Quigley and D. R. Bourne, *J. Less-Common Met.*, 170 (1991) 191.
- 3 I. J. McColm, *J. Solid State Chem.* (1992), to be published.
- 4 I. J. McColm, *J. Alloys Comp.*, 189 (1992) 31.
- 5 I. J. McColm, *J. Less-Common Met.*, 78 (1981) 287.
- 6 D. W. Jones, I. J. McColm and J. Yerkess, *J. Solid State Chem.*, 92 (1991) 301.
- 7 K. A. Gschneidner, Jr., *J. Less-Common Met.*, 25 (1971) 405.